

EFFECTS OF RADIATION ON CONVECTION HEAT TRANSFER OF Cu-WATER NANOFLUID PAST A MOVING WEDGE

by

Faiza A. SALAMA^{a,b}

^a Department of Mathematics, Faculty of Science and Arts, Qassim University,
Al-Muznib, Saudi Arabia

^b Department of Mathematics, Faculty of Science, Suez Canal University, Egypt

Original scientific paper

DOI: 10.2298/TSCI140719049S

Heat transfer characteristics of a 2-D steady hydrodynamic flow of water-based copper nanofluid over a moving wedge, taking into account the effects of thermal radiation, have been investigated numerically. The Rosseland approximation is used to describe the radiative heat flux in the energy equation. The governing fundamental equations are first transformed into a system of ordinary differential equations and solved numerically by using the fourth-order Runge-Kutta method with shooting technique. A comparison with previously published work has been carried out and the results are found to be in good agreement. The existence of unique and dual solutions for self-similar equations of the flow and heat transfer are analyzed numerically. The results indicate that there is strong dependence of the thermal gradient at the surface of the wedge on both velocity ratio parameter and thermal radiation.

Key words: *nanofluid, dual solution, thermal radiation*

Introduction

The study of convective heat transfer in nanofluids is gaining a lot of attentions. Nanofluids are suspensions of metallic (for example Cu, Al, Fe, Hg, Ti, *etc.*) or non-metallic (for example Al₂O₃, CuO, SiO₂, and TiO₂) nano-powders in base fluid (water, engine oil, ethylene glycol, *etc.*). The term *nanofluid* was first used by Choi [1]. He defined them as fluids containing particles of sizes below 100 nm. Nanofluids have novel properties that make them potentially useful in many applications in heat transfer, including microelectronics, fuel cells, pharmaceutical processes, and hybrid-powered engines. The broad range of current and future applications involving nanofluids have been given by Wong and Leon [2].

The characteristics feature of nanofluids is thermal conductivity enhancement, a phenomenon observed by Masuda *et al.* [3]. This makes nanofluids attractive for numerous engineering applications as in chemical production, production of microelectronic, automotives, power generation in a power plant, and advanced nuclear systems [4]. Many researchers have studied and reported results on convective heat transfer in nanofluids considering various flow conditions in different geometries, [5-11]. A comprehensive study of convective transport in nanofluids was made by Buongiorno [12]. Kuznetsov and Nield [13] presented a similarity solution of natural convective boundary-layer flow of a nanofluid past a vertical plate. Abu-Nada and Oztop [14] investigated numerically the effect of Cu-water nanofluid on

natural convection heat transfer in inclined cavity. They used the inclination angle as a control parameter for flow and heat transfer in the cavity. Khan and Pop [15] analyzed the boundary-layer flow of nanofluid past a stretching sheet. Hag *et al.* [16] investigated the effects of magnetohydrodynamic and volume fraction of carbon nanotubes (CNT) on the flow and heat transfer in two lateral directions over a stretching sheet. The MHD boundary layer flow of a Casson nanofluid over an exponentially permeable shrinking sheet with convective boundary condition was studied by Hag *et al.* [17]. Several researchers have recently investigated the problem of boundary layer flow in order to obtain the thermal and kinetic behavior by considering the different forms of stretching velocity and temperature profiles [18-20].

At high temperatures, thermal radiation can significantly effect the heat transfer and the temperature distribution in the boundary layer flow of participating fluid. Thermal radiation effects may play an important role in controlling heat transfer in industry where the quality of the final product depends on heat controlling factors to some extent. Recently, the effect of chemical reaction and heat radiation in the presence of a nanofluid flowing past porous vertical stretching surface was investigated by Rosmila *et al.* [21]. Hady *et al.* [22] analyzed the problem of boundary-layer flow and heat transfer in viscous nanofluid over a non-linearly stretched non-isothermal moving flat surface in the presence or absence of thermal radiation using the Rosseland approximation for radiative heat flux. Nadeem and Hag [23, 24] reported a numerical solution of the boundary layer nanofluid flow over a stretching/shrinking sheet with thermal radiation. Hag *et al.* [25] recently considered the effects of thermal radiation and slip velocity on MHD stagnation flow of nanofluid over a stretching sheet.

The boundary layer flow over a static or moving wedge in nanofluid has been considered by Yacob *et al.* [26], which is an extension of the flow over a static wedge considered by Falkner and Kan [27]. They employed a similarity transformation that reduces the partial differential boundary layer equations to a non-linear third-order ordinary differential equation before solving it numerically. Motivated by the work done in Yacob *et al.* [26], the present paper will study the Falkner-Skan boundary-layer problem for a moving wedge immersed in Cu-water nanofluid in the presence of thermal radiation. Using similarity transformations, the

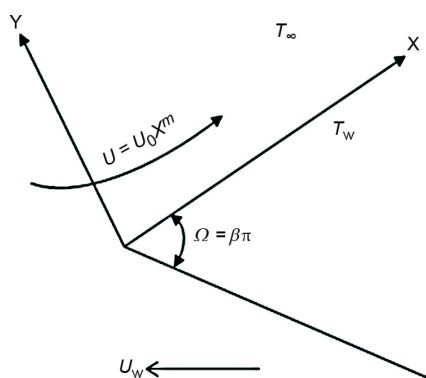


Figure 1. Physical model and the co-ordinate system

governing partial differential equations are reduced to a set of coupled non-linear ordinary differential equations with corresponding boundary conditions. The effects of the physical parameters of the problem such as velocity ratio, solid volume fraction, and thermal radiation, have been investigated in this problem.

Formulation of the problem

We consider the steady 2-D laminar boundary-layer flow of an incompressible viscous nanofluid (Cu-water) of density ρ_{nf} and temperature T_∞ moving over a wedge moving with the velocity $u_w(x)$. The positive x co-ordinate is measured along the surface of the wedge with the apex as origin, and the positive y co-ordinate is measured normal to the x-axis in the outward direction towards the fluid, fig. 1. It is assumed that the base fluid and the nanoparticles are in thermal equilibrium and no slip occurs between them. The thermophysical properties of the fluid and nanoparticles are given in tab. 1 [28]. Thermal radiation is included in the energy

equation. The governing partial differential equations for the boundary-layer flow of nanofluid, in this problem can be written [29]:

$$\frac{\partial u}{\partial x} + \frac{\partial v}{\partial y} = 0 \quad (1)$$

$$u \frac{\partial u}{\partial x} + v \frac{\partial u}{\partial y} = u_e(x) \frac{\partial u_e(x)}{\partial x} + \frac{\mu_{nf}}{\rho_{nf}} \frac{\partial^2 u}{\partial y^2} \quad (2)$$

$$u \frac{\partial T}{\partial x} + v \frac{\partial T}{\partial y} = \alpha_{nf} \frac{\partial^2 T}{\partial y^2} - \frac{1}{(\rho c_p)_{nf}} \frac{\partial q_r}{\partial y} \quad (3)$$

Table 1. Thermophysical properties of the base fluid and the nanoparticles

Physical properties	Fluid phase (water)	Cu
c_p [Jkg ⁻¹ K ⁻¹]	4179	385
ρ [kgm ⁻³]	997.1	8933
k [Wm ⁻¹ K ⁻¹]	0.613	400
$\alpha \cdot 10^7$ [m ² s ⁻¹]	1.47	1163.1

where u and v are velocity components along x- and y-axes, respectively, $u_e(x)$ – the velocity of the flow external to the boundary-layer, ρ_{nf} and μ_{nf} – the density and effective viscosity of nanofluid, respectively, α_{nf} and ν_{nf} – the thermal diffusivity and kinematic viscosity, respectively, which are defined [30]:

$$\nu_{nf} = \frac{\mu_{nf}}{\rho_{nf}}, \quad \rho_{nf} = (1 - \varphi)\rho_f + \varphi\rho_s, \quad \mu_{nf} = \frac{\mu_f}{(1 - \varphi)^{2.5}}, \quad \alpha_{nf} = \frac{k_{nf}}{(\rho c_p)_{nf}},$$

$$\rho c_p = (1 - \varphi)(\rho c_p)_f + \varphi(\rho c_p)_s, \quad \frac{k_{nf}}{k_f} = \frac{(k_s + 2k_f) - 2\varphi(k_f - k_s)}{(k_s + 2k_f) + 2\varphi(k_f - k_s)} \quad (4)$$

where φ is the solid volume fraction of nanofluid, μ_f – the viscosity of the basic fluid, ρ_f and ρ_s – the densities of the pure fluid and nanoparticle, respectively, $(\rho c_p)_f$ and $(\rho c_p)_s$ – the specific heat parameters of the basic fluid and nanoparticle, respectively, and k_f and k_s are the thermal conductivities of the basic fluid and nanoparticle, respectively.

Using Rosseland approximation for radiation [31] we can write:

$$q_r = - \frac{4\sigma}{3k^*} \frac{\partial T^4}{\partial y} \quad (5)$$

where σ is the Stefan-Boltzman constant, and k^* – the absorption coefficient.

Assuming that the temperature difference within the flow is such that T^4 may be expanded in a Taylor series and expanding T^4 about T_∞ and neglecting higher orders we get $T^4 = 4T_\infty^3 T - 3T_\infty^4$. Now eq. (3) becomes:

$$u \frac{\partial T}{\partial x} + v \frac{\partial T}{\partial y} = \alpha_{nf} \frac{\partial^2 T}{\partial y^2} - \frac{16\sigma T_\infty^3}{3k^*(\rho c_p)_{nf}} \frac{\partial^2 T}{\partial y^2} \quad (6)$$

The appropriate boundary conditions for the problem are given by:

$$u = u_w(x) = U_w x^m, \quad v = 0, \quad T = T_w \quad \text{at} \quad y = 0$$

$$u = u_e(x) = U_0 x^m, \quad T \rightarrow T_\infty \quad \text{as} \quad y \rightarrow \infty \quad (7)$$

where $m = \beta(2 - \beta)$, and β is the Hartree pressure gradient parameter that corresponds to $\beta = \Omega/\pi$ for a total angle Ω of the wedge, U_w and U_0 are constants. We notice that $0 \leq m \leq 1$, with $m = 0$ for the flow over a moving flat plate, and $m = 1$ for the flow near the stagnation point on a moving wall.

Now we introduce the following similarity variables:

$$\psi = \left[\frac{2\nu_f x u_e(x)}{m+1} \right]^{\frac{1}{2}} f(\eta), \quad \eta = \left[\frac{(m+1)u_e(x)}{2\nu_f x} \right]^{\frac{1}{2}} y, \quad \theta = \frac{T - T_\infty}{T_w - T_\infty} \quad (8)$$

where ψ is the stream function and is defined in the usual way as $u = \partial\psi/\partial y$ and $v = -(\partial\psi/\partial x)$, so as to identically satisfy eq. (1), and ν_f is the kinematic viscosity of the fluid. Substituting eq. (8) into eqs. (2) and (6), we get the following non-linear ordinary differential equations:

$$f''' + (1 - \varphi)^{2.5} \left(1 - \varphi + \varphi \frac{\rho_s}{\rho_f} \right) \left[ff'' + \frac{2m}{m+1} (1 - f'^2) \right] = 0 \quad (9)$$

$$\left(\frac{k_{nf}}{k_f} + \frac{4}{3R} \right) \theta'' + \text{Pr} \left[1 - \varphi + \varphi \frac{(\rho c_p)_s}{(\rho c_p)_f} f \theta' \right] = 0 \quad (10)$$

Subject to the boundary conditions:

$$\begin{aligned} f(\eta) = 0, \quad f'(\eta) = \lambda, \quad \theta(\eta) = 1 \quad \text{at} \quad \eta = 0, \\ f'(\eta) = 1, \quad \theta(\eta) = 0 \quad \text{as} \quad \eta \rightarrow \infty \end{aligned} \quad (11)$$

where prime denotes differentiation with respect to η , $\text{Pr} = \nu_f/\alpha_f$ is the Prandtl number, and $R = k_{nf}k^*/4\sigma T_\infty^3$ is the radiation parameter, $\lambda = U_w/U_0$ – the ratio of the wall velocity to the free stream fluid velocity, $\lambda(> 0)$ corresponds to the situation when the wedge moves in the same direction to the free stream and $\lambda(< 0)$ when the wedge moves in the opposite direction to the free stream, while $\lambda = 0$ corresponds to a static wedge. If $\varphi = 0$ (Newtonian fluid), eq. (9) reduces to the problem studied by Falkner and Skan [27].

Important physical parameters for this flow and heat transfer situations are the local skin-friction coefficient and the local Nusselt number which are defined by:

$$c_f = \frac{\tau_w}{\rho_f [u_e(x)]^2} \quad \text{and} \quad \text{Nu}_x = \frac{xq_w}{k_f(T_w - T_\infty)} \quad (12)$$

where

$$\tau_w = \mu_{nf} \left[\frac{\partial u}{\partial y} \right]_{y=0} \quad \text{and} \quad q_w = -k_{nf} \left[\frac{\partial T}{\partial y} - q_r \right]_{y=0}$$

are shear stress and surface heat flux respectively. Using the new similarity variables in eq. (8) gives:

$$c_f \left[\frac{2 \text{Re}_x}{m+1} \right]^{1/2} = \frac{1}{(1 - \varphi)^{2.5}} f''(0) \quad \text{and} \quad \text{Nu}_x \left[(m+1) \frac{\text{Re}_x}{2} \right]^{-1/2} = -\frac{k_{nf}}{k_f} \left(1 + \frac{4}{3R} \right) \theta'(0) \quad (13)$$

where $\text{Re}_x = u_e x/\nu_f$ is the local Reynolds number.

Numerical procedure

Equations (9) and (10) along with the boundary conditions (11) constitute a one-parameter two-point boundary value problem. The ordinary differential equations were written as a system of five coupled first-order equations in terms of five dependent variables z_n ($n = 1, 2, \dots, 5$), where $z_1 = f, z_2 = f', z_3 = f'', z_4 = \theta$, and $z_5 = \theta'$. Thus:

$$\begin{aligned}
 z_1' &= z_2, & z_1(0) &= 0 \\
 z_2' &= z_3, & z_2(0) &= \lambda \\
 z_3' &= -(1 - \varphi)^{2.5} \left(1 - \varphi + \varphi \frac{\rho_s}{\rho_f} \right) \left[z_1 z_3 + \frac{2m}{m+1} (1 - z_2^2) \right], & z_3(0) &= \alpha_1 \\
 z_4' &= z_5, & z_4(0) &= 0 \\
 z_5' &= \frac{-p_r \left[1 - \varphi + \varphi \frac{(\rho c_p)_s}{(\rho c_p)_f} - z_1 z_5 \right]}{\frac{k_{nf}}{k_f} + \frac{4}{3R}}, & z_5(0) &= \alpha_2
 \end{aligned}$$

where α_1 and α_2 are determined such that $z_2(\infty) = 1$ and $z_4(\infty) = 0$. The essence of this method is the reduction of the boundary value problem to an initial value problem and then use a shooting numerical technique [31] to guess α_1 and α_2 until the boundary condition $z_2(\infty) = 1$ and $z_4(\infty) = 0$ are satisfied. The resulting differential equations are then easily integrated using fourth-order classical Runge-Kutta method.

Results and discussion

The effects of the solid volume fraction of the nanofluid φ , the radiation parameter R , and the moving wedge parameter λ are analyzed for one type of nanoparticle, namely Cu-water, as the working fluid. In the absence of thermal radiation, in order to validate our method, we compare the values of $f''(0)$ with the results obtained by Rosenhead [32], Watanabe [33], Yih [34], and Yacob *et al.* [26] for different values of m when $\lambda = 0$ (fixed wedge) and $\varphi = 0$ (regular fluid). This comparison is illustrated in tab. 2 and it shows a very favorable agreement. Therefore, we are confident that the results obtained in this paper are accurate.

Table 2. Comparison of the value of $f''(0)$ for various of m with $\lambda = \varphi = 0$ and $R \rightarrow \infty$

m	Rosenhead [32]	Wathanabe [33]	Yih [34]	Yacob [26]	Present result
0		0.46960	0.469600	0.4696	0.4695614
1/11		0.65498	0.654979	0.6550	0.6549213
0.2		0.80213	0.802125	0.8021	0.8012192
0.13		0.92765	0.927653	0.9277	0.9269235
0.5				1.0389	1.038876
1	1.232588		1.232588	1.2326	1.2283297

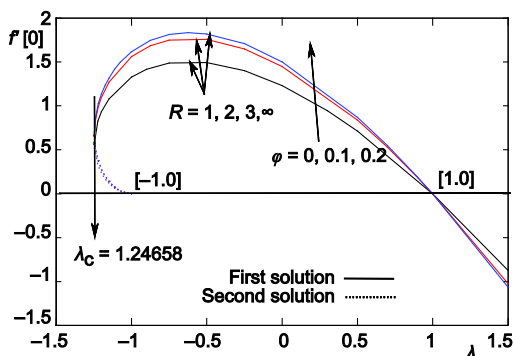


Figure 2. Shear stress vs. λ for various values of R and ϕ when $m = 1$

where λ_c is the critical value having a single solution for this problem. Since radiation parameter does not occur explicitly in the momentum equation, its effect on the wall shear stress $f''(0)$ is negligible, as shown in fig. 2. It is also observed that, for all values of R and ϕ in this study, the wall shear stress is positive when $\lambda < 1$ and it becomes negative when $\lambda > 1$. It can also be seen in fig. 2 that, as expected, all the solutions pass through $f''(0) = 0$ when $\lambda = 1$, and corresponding velocity curve has a horizontal tangent inside the boundary layer (fig. 5). Physically, this point corresponds to zero friction in the boundary layer because the wedge and the fluid move with the same velocity. This observation is in agreement with that obtained by

Variation of the wall shear stress $f''(0)$ and the wall heat transfer $-\theta'(0)$ with λ for $m = 1$, $Pr = 6.2$ (water) and different values of the thermal radiation parameter R and the solid volume fraction nanoparticle parameter ϕ with Cu-water nanofluid are presented in figs. 2-4. These figures show that the existence and uniqueness of solution depend on the velocity ratio parameter λ . Also, it is observed that the solution is unique when $\lambda > -1$, there exists dual solutions for $\lambda_c < \lambda < -1$ and for $\lambda < \lambda_c$, the boundary layer theory breaks down and eqs. (9) and (10) become unsolvable. Based on our computations, $\lambda_c = -1.24658$ when $m = 1$, $R = 1, 2, 3, \infty$, and $\phi = 0, 0.1, 0.2$,

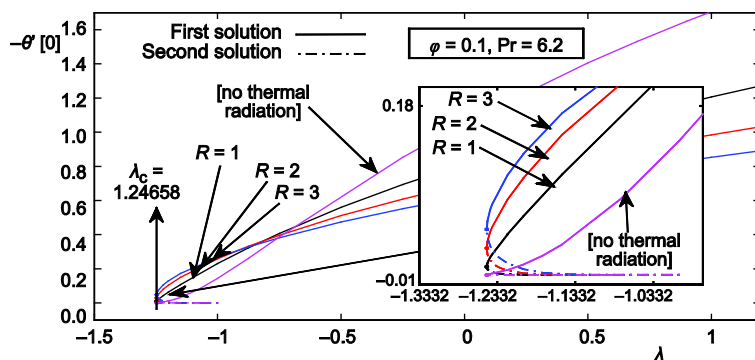


Figure 3. Temperature gradient vs. λ for various values of R when $m = 1$

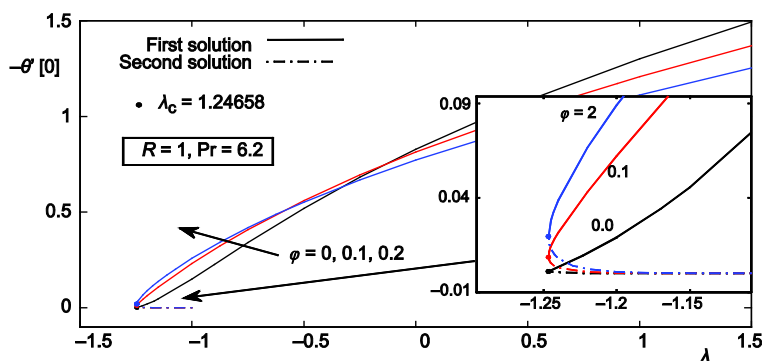


Figure 4. Temperature gradient vs. λ for various values of ϕ when $m = 1$

Yacob *et al.* [26]. The values of temperature gradient at the wall $-\theta'(0)$ are plotted in figs. 3 and 4 for different values of R and ϕ , respectively. From both figures is noticed the dual solutions existing in the range of λ as previously stated. The wall heat transfer $-\theta'(0)$ increases with increasing values of λ in the case of first solution (solid lines) and decreases for second solution (dashed lines), except for the case of regular fluid ($\phi = 0$) and absence of thermal radiation ($R \rightarrow \infty$). With increasing values of R and ϕ the wall heat transfer for first and second solutions also increase inside the boundary layer while reverse behavior is observed for the unique wall heat transfer profiles ($\lambda > -1$).

Figures 5 and 6 show the variation of the velocity and temperature profiles for different values of the velocity ratio parameters λ when $R = 1$ and $\phi = 0.1$, respectively. From these two figures, we observe that for the case of dual solution, the momentum and thermal boundary layer thicknesses for the first solution are thinner than that of second solution and the first solution is likely to be the physical and stable solution. The unique solution of velocity profile for $\lambda > -1$ increases with increasing λ . However, the velocity profiles are constant and the shear stress is zero for $\lambda = 1$. This is because the wedge velocity is equal to the free stream velocity. For $\lambda_c < \lambda \leq -1$, it is found that the first solution of velocity profiles (dash-dotted lines) exhibit the identical characters as that of the velocity profiles for unique solution and reverse nature is noticed for the case of the second solution (dotted lines). The inset shows that the stream function $f(\eta)$ increases with η or positive values of λ . For $\lambda = 1$, the stream function becomes linear. Physically this point corresponds to zero friction in the boundary layer. For negative values of λ , the stream function becomes negative over an increasing range of η but for larger values of η , it becomes increasing *i. e.* the region of reverse flow appears here. This is because the wedge and the free stream move in opposite direction. From fig. 6 it is found that the value of the temperature profile decreases for an increase of λ in the first solution (dash-dotted lines) and it decreases for the second solution (dotted lines). Also, the behavior of unique solution of temperature profiles (dashed lines) is similar to the profiles of the first solution in the same figure.

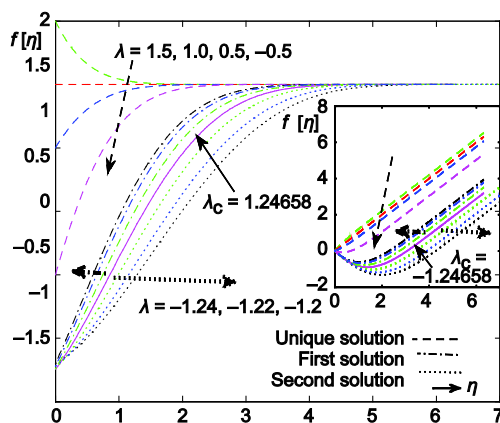


Figure 5. Velocity profile for various values of λ when $R = 1$, $\phi = 0.1$, and $m = 1$

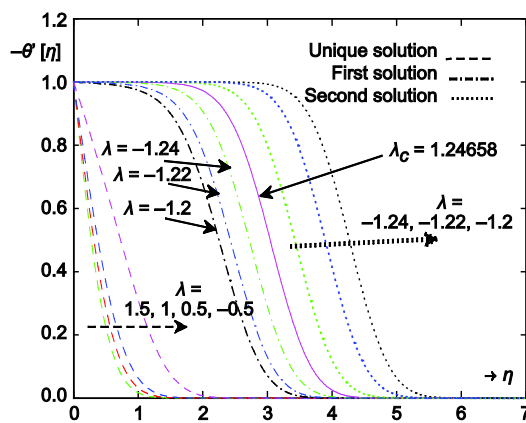


Figure 6. Temperature profile for various values of λ when $R = 1$, $\phi = 0.1$, and $m = 1$

Figures 7-9 show the effect of radiation parameter on the velocity, temperature and temperature gradient profiles for two values of $\lambda = 1.2$, and -1.2 with $\phi = 1$. From fig. 7, it is obvious that the radiation parameter has a negligible effect on the velocity profiles since the

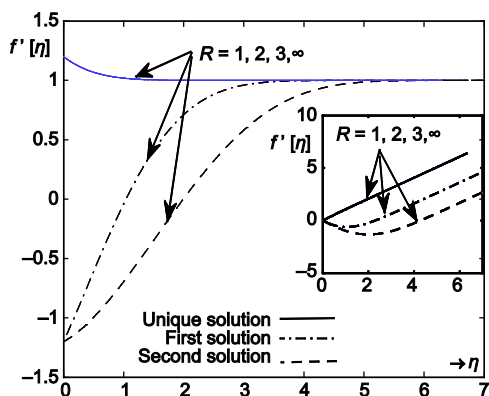


Figure 7. Velocity profile for various values of R when $\varphi = 0.1$, and $m = 1$

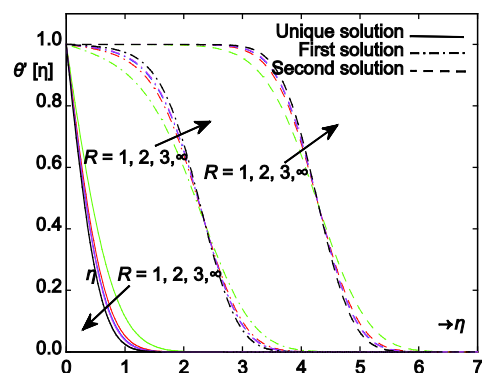


Figure 8. Temperature profile for various values of R when $\varphi = 0.1$, and $m = 1$

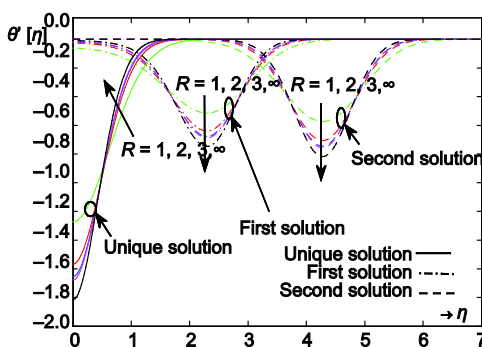


Figure 9. Temperature gradient for various values of R when $\varphi = 0.1$, and $m = 1$

parameter R is associated basically with the energy equation. This observation is consistent to the variation of $f''(0)$ presented in fig. 2. The results of temperature profiles at $\lambda = 1.2$ and -1.2 under different values of radiation parameter R are shown in fig. 8. It is found that for $\lambda = 1.2$, there is only a unique solution and the temperature profiles inside the thermal boundary layer are decreasing with an increase of radiation parameter. However, different behavior appears when $\lambda = -1.2$. In this case, there are two solutions of temperature profiles; for both solutions, the temperature profiles have crossover points for different values of radiation parameter R . The first solution of temperature profile increases with an increase in R within the thermal boundary layer and the reverse is seen away from the surface, till it reaches the value of $\theta(0)$ as $\eta \rightarrow \infty$. It is noted that, far away from the surface, the second temperature profiles exhibit the identical characters as that of the temperature profile for the first solution. We can also see that, the temperature is high within the boundary layer with low value of radiation parameter. For $\lambda = -1.2$, the temperature inside the thermal boundary layer is high with high value of R , while outside the thermal boundary layer, the temperature is low with high value of R in the first solution. A similar behavior has also been observed far away from the surface in the case of second solution.

From fig. 9, for $\lambda = 1.2$, temperature gradient profile is negative (reversed heat flow), with its maximum magnitude at $\eta = 0$. In addition, its magnitude decreases within the boundary layer as R increases, whereas a reverse trend is seen away from the surface, till it reaches the value of $\theta'(\eta_\infty) = 0$, where η_∞ is relatively small. For $\lambda = -1.2$ (the wedge and the free stream velocity move in the opposite direction), we have found that, there are two solutions of the temperature gradient profiles which are different from those obtained for $\lambda = 1.2$ (the wedge and the free stream velocity move in the same direction).

The first solution of temperature gradient initially increases with R within the thermal boundary layer, after that it starts decreasing to the minimum before increasing to zero at η_∞ , where the minimum value decreases as R increases and η_∞ is now relatively large. A similar

Table 3. Values of $f''(0)$ and $-\theta'(0)$ for various of R when with $\lambda = -1.2$, $\phi = 0.1$, and $Pr = 6.2$

R	$[2Re_x/(m+1)]^{1/2}C_f$		$[(m+1)2Re_x/2]^{-1/2}Nu_x$	
	first solution	second solution	first solution	second solution
1	1.0954190	0.27447918	0.0621899	0.0001345
2	1.0954190	0.27447918	0.1029498	0.0017645
3	1.0954190	0.27447918	0.1287283	0.0060823
4	1.0954190	0.27447918	0.1450409	0.0124140

behavior has also been observed for larger values of η_∞ in the case of second solution. In figs. 10 and 11, the effect of volume fraction of nanoparticles ϕ on the velocity and temperature profiles are, respectively, presented for two values of the velocity ratio parameter λ 1.2, and -1.2 with $R = 1$. It may be noted that the decrease in ϕ causes a reduction in momentum boundary layer for the first solution as well as the second solution. A reverse trend is seen in the case of unique solution. This is because the fluid and the surface move in the same direction. Also, it is observed that the increase in ϕ causes a reduction in thermal boundary layer for first and second solutions. On the contrary, the decrease in ϕ causes a reduction in thermal boundary layer for unique solution. The results indicate that the momentum and thermal boundary layer thicknesses for the unique and the first solutions are thinner than those of the second solution. Finally, the values of the skin friction coefficient and Nusselt number for $R = 1, 2, 3$, and 4 when $\lambda = -1.2$, $\phi = 0.1$, and $Pr = 6.2$ are given in tab. 3. It is observed that the radiation parameter has no effect on the skin friction coefficient whereas it increases the Nusselt number throughout the thermal boundary layer.

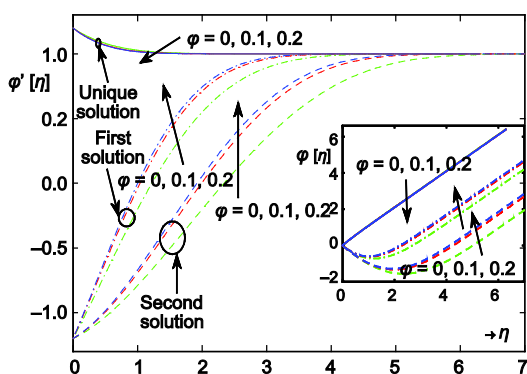


Figure 10. Velocity profile for various values of ϕ when $R = 1$ and $m = 1$

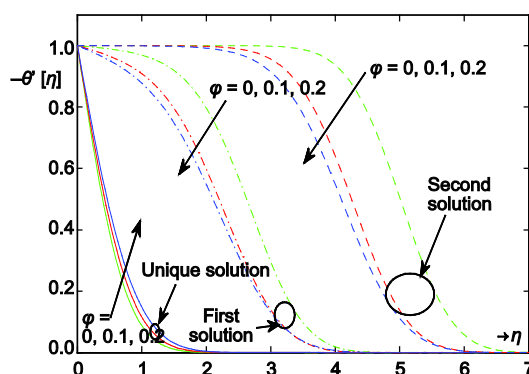


Figure 11. Temperature profile for various values of ϕ when $R = 1$ and $m = 1$

Conclusions

The present study deals with the numerical solutions for steady 2-D boundary layer flow past a moving wedge in a copper-water nanofluid numerically taking into account the effect of thermal radiation. The problem has been solved numerically to exhibit the effects of the physical parameters λ , R , and ϕ . Dual similarity solutions for velocity field and also for temperature distribution are obtained for some negative values of velocity ratio parameter. Also, the

solution does not exist beyond a certain critical value of λ . This critical value of λ does not depend on the values of radiation parameter. Boundary layer thicknesses (both momentum and thermal) for the first solution were thinner than that of second solution and the first solutions are stable and physically realizable while the second solution is not [35].

Combined effect of velocity ratio parameter and radiation parameter strongly controls the flow and heat transfer characteristics for a steady 2-D boundary layer past a moving wedge in a copper-water nanofluid.

Acknowledgments

The author would like to thank the anonymous reviewers for their comments and suggestions which led to the improvement of this paper.

References

- [1] Choi, S. U. S., Enhancing Thermal Conductivity of Fluids with Nanoparticles, *Proceedings*, ASME International Mechanical Engineering Congress and Exposition, ASME, FED 231/MD, San Francisco, Cal., USA, 1995, pp. 99-105
- [2] Wong, K. F. V., Leon, O. D., Applications of Nanofluids: Current and Future, *Adv. Mech. Eng.* 2010, (2010), ID 519659, p. 11
- [3] Masuda, H., *et al.*, Alteration of Thermal Conductivity and Viscosity of Liquid by Dispersing Ultra-Fine Particles, *Netsu Busei*, 7 (1993), 4, pp. 227-223
- [4] Buongiorno, J., Hu, W., Nanofluid Coolants for Advanced Nuclear Power Plants, Paper no. 5705, *Proceedings*, ICAPP, Seoul, 2005
- [5] Khanafer, K., *et al.*, Buoyancy-Driven Heat Transfer Enhancement in a Two-Dimensional Enclosure Utilizing Nanofluids, *Int. J. Heat Mass Transf.*, 46 (2003), 19, pp. 3639-3653
- [6] Maiga, S. E. B., *et al.*, Heat Transfer Enhancement by using Nanofluids in Forced Convection Flows, *Int. J. Heat Fluid Flow*, 26 (2005), 4, pp. 530-546
- [7] Jou, R. Y., Tzeng, S. C., Numerical Research of Nature Convective Heat Transfer Enhancement Filled with Nanofluids in Rectangular Enclosures, *Int. Commu. Heat Mass Transf.*, 33 (2006), 6, pp. 727-736
- [8] Tiwari, I. K., Das, M. K., Heat Transfer Augmentation in a Two-Sided Lid-Driven Differentially Heated Square Cavity Utilizing Nanofluids, *Int. J. Heat Mass Trans.*, 50 (2007), 9-10, pp. 2002-2018
- [9] Hwang, K. S., *et al.*, Buoyancy-Driven Heat Transfer of Water-Based Nanofluids in a Rectangular Cavity, *Int. J. Heat Mass Transf.*, 50 (2007), 19-20, pp. 4003-4010
- [10] Oztop, H. F., Abu-Nada, E., Numerical Study of Nature Convection in Partially Heated Rectangular Enclosures Field with Nanofluids, *Int. J. Heat Fluid Flow*, 29 (2008), 5, pp. 326-336
- [11] Muthamilselvan, M., *et al.*, Heat Transfer Enhancement of Copper-Water Nanofluids in a Lid-Driven Enclosure, *Commun. Non-linear Sci. Numer. Simulat.*, 15 (2010), 6, pp. 1501-1510
- [12] Buongiorno, J., Convective Transport in Nanofluids, *ASME J. Heat transfer*, 128 (2006), 3, pp. 240-250
- [13] Kuznetsov, A. V., Nield, D. A., Natural Convective Boundary-Layer Flow of a Nanofluid Past Vertical Plate, *Int. J. Therm. Sci.*, 49 (2010), 2, pp. 243-247
- [14] Abu-Nada, E., Oztop, H. F., Effects of Inclination Angle on Natural Convection in Enclosures Filled with Cu-Water Nanofluid, *Int. J. of Heat and Fluid Flow*, 30 (2009), 4, pp. 669-678
- [15] Khan, W. A., Pop, I., Boundary-Layer Flow of a Nanofluid Past a Stretching Sheet, *Int. Journal of Heat and Mass Transfer*, 53 (2010), 11-12, pp. 2477-2483
- [16] Hag, R. U., *et al.*, A., Thermophysical Effects of Carbon Nanotubes on MHD Flow over a Stretching Surface, *Physica E: Low-Dimensional Systems and Nanostructures*, 63 (2014), Sep., pp. 215-222
- [17] Hag, R. U., *et al.*, Convective Heat Transfer and MHD Effects on Casson Nanofluid Flow over a Shrinking Sheet, *Journal Central European Journal of Physics*, 12 (2014), 12, pp. 862-871
- [18] Nadeem, S., *et al.*, Heat Transfer Analysis of Water-Based Nanofluid over an Exponentially Stretching Sheet, *Alexandria Engineering Journal*, 53 (2014), 1, pp. 219-224
- [19] Nadeem, S., *et al.*, Numerical Study of MHD Boundary Layer Flow of a Maxwell Fluid Past a Stretching Sheet in the Presence of Nanoparticles, *Journal of the Taiwan Institute of Chemical Engineers*, 45 (2014), 1, pp. 121-126
- [20] Nadeem, S., *et al.*, Numerical Solution of Non-Newtonian Nanofluid Flow over a Stretching Sheet, *Applied Nanoscience*, 4 (2014), 5, pp. 1-7

- [21] Rosmila, A.-K., *et al.*, Scaling Group Transformation for Boundary-Layer Flow of a Nanofluid Past a Porous Vertical Stretching Surface in the Presence of Chemical Reaction with Heat Radiation, *Comput. Fluids*, 25 (2011), Dec., pp. 15-21
- [22] Hady, F. M., *et al.*, Radiation Effect on Viscous Flow of a Nanofluid and Heat Transfer over a Non-Linearly Stretching Sheet, *Nanoscale Research Letters*, 7 (2012), Dec., pp. 229-232
- [23] Nadeem, S., Hag, R. U., MHD Boundary Layer Flow of a Nano Fluid Past a Porous Shrinking with Thermal Radiation, *Journal of Aerospace Engineering*, 28 (2015), 2, 04014061
- [24] Nadeem, S., Hag, R. U., Effect of Thermal Radiation for Magneto hydrodynamic Boundary Layer Flow of a Nanofluid Past a Stretching Sheet with Convective Boundary Conditions, *Journal of Computational and Theoretical Nanoscience*, 11 (2013), 1, pp. 32-40
- [25] Hag, R. U., *et al.*, Thermal Radiation and Slip Effects on MHD Stagnation Point Flow of Nanofluid over a Stretching Sheet, *Physica E: Low-Dimensional Systems and Nanostructures*, 65 (2015), Jan., pp. 17-23
- [26] Yacob, N. A., *et al.*, Falkner-Skan Problem for a Static or Moving Wedge in Nanofluids, *Int. J. of Thermal Science*, 50 (2011), 2, pp. 133-139
- [27] Falkner, V. M., Skan, S. W., Some Approximate Solutions of Boundary Layer Equations, *Philosophical Magazine and Journal of Science*, 12 (1931), 80, pp. 865-896
- [28] Oztop, H. F., Abu-Nada, E., Numerical Study of Natural Convection in Partially Heated Rectangular Enclosures Filled with Nanofluids, *Int. J. Heated Fluid Flow*, 29 (2008), 5, pp. 1326-1336
- [29] Tiwari, R. J., Das, M. K., Heat Transfer Augmentation in a Two-Sided Lid-Driven Differentially Heated Square Cavity Utilizing Nanofluids, *Int. J. Heat Mass Transfer*, 50 (2007), 9-10, pp. 2002-2018
- [30] Khanafer, R., Lightstone, M., Buoyancy-Driven Heat Transfer Enhancement in a Two-Dimensional Enclosure Utilizing Nanofluids, *Int. J. Heat Mass Transfer*, 46 (2003), 19, pp. 3639-3653
- [31] Na, T. Y., *Computational Method in Engineering Boundary Value Problems*, Academic Press, New York, N. Y., USA, 1979
- [32] Rosenhead, L., *Laminar Boundary Layer*, Oxford University Press, Oxford, UK, 1963
- [33] Watanabe, T., Thermal Boundary Layers over a Wedge with Uniform Suction or Injection in Forced Flow, *Acta Mech.*, 83 (1990), 3, pp. 119-126
- [34] Yih, K. A., Uniform Suction (Blowing) Effect on Forced Convection about a Wedge: Uniform Heat Flux, *Acta Mech.*, 128 (1998), 3, pp. 173-181
- [35] Bachok, N., *et al.*, The Boundary Layers of an Unsteady Stagnation-Point Flow in Nanofluid, *Int. J. of Heat and Mass Trans.*, 55 (2012), 23-24, pp. 6499-6505

